This article has been accepted for publication in a future issue of this journal, but has not been fully edited. Content may change prior to final publication. Citation information: DOI 10.1109/TPWRD.2019.2925622, IEEE Transactions on Power Delivery

Wall Fusion of Buried Pipelines due to Direct Lightning Strikes: Field, Laboratory and Simulation Investigation of the Damaging Mechanism

C.A. Charalambous, *Member, IEEE,* A. Dimitriou, N. Kioupis, T. Manolis and N. Kokkinos

***Abstract*— Wall fusion of buried pipelines can occur if the driving voltage and available current is sufficiently high. For example, it can occur from direct lightning strikes to earth, close to the pipelines' routing. However, not all factors for defining the energy discharge needed to fuse the pipe wall are thoroughly investigated or understood. This article enriches the ongoing research activities in an attempt to understand such detrimental damages. In particular, the paper formulates its research contents around a documented wall fusion incident on an underground Gas Transmission System, due to a nearby direct lightning strike. The investigation embraces field, laboratory and modelling activities to provide insights on the damaging mechanism. Of particular importance, in understanding this mechanism is the influence of soil ionization. To this end, a model is developed to investigate the soil-ionized flow of the lightning discharge current - into the pipeline's metal wall, through existing coating defects - thus revealing its detrimental effect.**

***Index Terms*—Gas Pipeline, Lightning, Soil Ionization, Coating Defect, Metal Fusion**

I. Introduction

THE belief that gas pipelines are effectively protected against direct lightning strikes - by virtue of their buried nature and modern coating layers - has been progressively revoked by some serious incidents [1]-[2]. Preliminary investigations to this extent, suggest that the impact of the lightning current discharge on buried pipeline primarily depends on the buried depth of the pipeline and on the distance of the pipeline to the lightning discharge location. However, foreseeing the exact impact is a complex problem, with multiple interacting variables. In the related scientific literature, the mechanisms through which lightning activity causes a failure (i.e. wall fusion) to buried pipelines are still, not fully investigated.

Although there is no simple criterion for defining a limit to the energy discharge needed to fuse the pipe wall, the AUS standard [3] documents, some parameters that are associated with such risk. The risk sources are reported to be the peak value of the lightning current, the charge of the lightning current (Q_{flash}) consisting of the charge of the short stroke (Q_{short}) and the charge of the long stroke (Q_{long}), the soil resistivity, the proximity of the pipelines' grounding systems to the lightning strike location, as well as the wall thickness of the pipeline.

However, there are other non-thoroughly investigated factors that may facilitate the flow of lightning discharge current into the pipeline metal. Such an example pertains to the influence of soil ionization (at the location of the lightning strike) on the pipeline's withstand capabilities - especially in the presence of existing coating defects in the section of the pipeline that falls within the formed soil ionization region. The latter has been given little or no attention, since the current knowledge [4]-[10] suggests that soil ionization will typically reduce the effective local resistivity around buried conductors and hence improve their grounding performance. Nonetheless, as it will be evidently discussed in this paper, soil ionization may, under certain conditions, act to facilitate the flow of lightning discharge current into the pipeline's metal through existing coating defects.

This paper manifests the quintessence of the above introductory remarks through the following structure: Section II describes a very recent metal wall fusion incident, on a high-pressure underground Gas Transmission System. This incident was caused by a direct lightning strike in the nearby vicinity of the pipeline. Section III, describes a series of laboratory experiments on specimens of the pipeline, which had suffered the metal wall fusion and gas leakage as a consequence. Finally, Section IV describes some state-of-the art modelling techniques and analysis to understand the mechanism that has caused this damage. It is highlighted that the discussion remarks in Section IV are not limited to the reported incident, but they are also generically extrapolated.

II. Brief Description of Reported Pipeline Damage

In mid-March 2017, there was a reported gas leakage and metal wall fusion on a secondary branch (100 km in length) of the high-pressure natural gas pipeline, of the Hellenic Gas Transmission System. The incident took place at the 52nd km (approximately) of this 100 km branch. An emergency field investigation, from the Gas Transmission System Operator has revealed that the cause of the wall fusion, was a direct lightning strike on a nearby small bush. The location of the lightning strike has been identified to be, at approximately 5 m away from

C. A. Charalambous, A. Dimitriou are with the Department of Electrical and Computer Engineering, Faculty of Engineering, of the University of Cyprus, PO Box 20537, 1687, Nicosia, Cyprus (e-mail of corresponding author: cchara@ucy.ac.cy).

N. Kioupis and T. Manolis are with the Hellenic Gas Transmission System Operator, DESFA Head Office 357 -359 Mesogeion Av. 152 31 Chalandri

N. Kokkinos is with ELEMKO SA, 90 TATOIOU Metamorphosis, 144 52, Greece

This article has been accepted for publication in a future issue of this journal, but has not been fully edited. Content may change prior to final publication. Citation information: DOI 10.1109/TPWRD.2019.2925622, IEEE Transactions on Power Delivery

the wall fusion location (See Fig.1). Moreover, the location of the lightning strike had also been reported/confirmed through the long-range lightning detection system of the National Observatory of Athens (NOA). The detection system is based on a network of six receivers located in Europe (ZEUS lightning detection system) [11]. The information registered on the incident's day, suggests that there was a lightning strike very near to the location (~ 60 m) of the pipeline's damage. Interestingly, two more lightning strikes had been also registered near (~ 200 m) to the location of the damage, however earlier in the month.

To facilitate a comprehensive overview of the underlying physical conditions, infrastructure's characteristics as well as to highlight the findings - of the thorough field investigation carried out by the transmission operator – the following information (*A, B*) is documented.

Fig.1 Pictures associated with Field Investigation and Findings

A. Pipeline Design and Material Characteristics

The inquired pipeline is a branch that diverts from the main Gas Transmission Line. This branch has a total length of 100 km. The characteristics of the pipeline are given in Table I.

TABLE I
PIPELINE CHARACTERISTICS

Pipeline wall resistivity (relative to annealed copper)	10
Pipeline wall permeability (relative to free space)	250
Pipeline coating resistivity	10^9 Ωm
Coating thickness	0.005 m
Pipeline radius	0.381 m
Wall thickness	10 mm
Buried Depth (upper edge at the location of the damage)	1.25 m

Moreover, the whole of the 100 km branch embraces 103 earthing mitigation wires. These had been installed to eliminate the effects of long and short term Electromagnetic Interference from adjacent power lines in the pipeline's right of way. These electrodes are continuous hot dip galvanized steel stay wires. The minimum external diameter of the wires is 12 mm that includes a 70 μm layer of zinc (500 g/m^2). They are installed at the same level and in parallel to the pipeline routing, through dc decoupling devices equipped with Transient Voltage Suppressors (TVS). The nearest earthing wires, to the damage location (i.e. 52nd km), are installed at 48,074 km (electrode length 135 m) and at 61.61 km (electrode length 110 m). Additionally, the pipeline is grounded at its 54.56 km through a 20 × 20 m grid. This grid is associated with a valve station.

It is also important to specify that within the 100 km of the sector, there exist three insulation joints. These are installed at 0 km, 61.34 km and 100 km respectively. The insulation joints are protected by spark-gap devices (details shown in Table II).

TABLE II
SPARK-GAP DEVICES - CHARACTERISTICS

Nominal discharge current (8/20 μs) I_n	100 kA
Lightning Impulse current (10/350 μs) I_{imp}	50 kA
Rated impulse spark over voltage (1,2/50 μs) U_{rimp}	≤ 2,2 kV

Finally, at the area near the location of the damage, some soil resistivity measurements (see Table III) were performed soon after the reported gas leakage incident. These measurements were obtained using the standard Wenner Method, at various depths across four different axis.

TABLE III
SOIL RESISTIVITY MEASUREMENTS

Measurement depth "a" (m)	**Soil resistivity "ρ" (Ωm)**			
	Axis 1	**Axis 2**	**Axis 3**	**Axis 4**
1	784	733	790	681
2	1100	1051	1011	959
4	1248	1193	1209	1300
8	1431	1507	1411	1007
16	1523	1667	1679	1621

By taking into consideration the available measurement data (Table III) and by the use of software [12], a resulting representative three-layer soil model, shown in Table IV, has been concluded.

TABLE IV
EQUIVALENT THREE-LAYER SOIL MODEL

Layer	**Soil resistivity "ρ" (Ωm)**	**Thickness (m)**
Upper	630.47 Ω m	0.94 m
Middle	1239.93 Ω m	0.2 m
Lower	1535.51 Ω m	Infinite Depth
Note: The rms error between measured and calculated resistivities was 11.02%.		

B. Field Investigation and Findings

Soon after the reported incident, the system operator has carried out a thorough field investigation that included the excavation of a pipeline's sector (see Fig.1) near the location of the damage. The main findings of this investigation are reported in Fig. 2. In particular, Fig. 2 shows a single line diagram of the excavated section. This section is 12m in length (i.e. between two welded joints). Within, this section, five locations with evident marks of coating and pipe wall damage had been identified. The exact locations of the damages are shown in Fig. 2 with reference to the circumference of the pipeline.

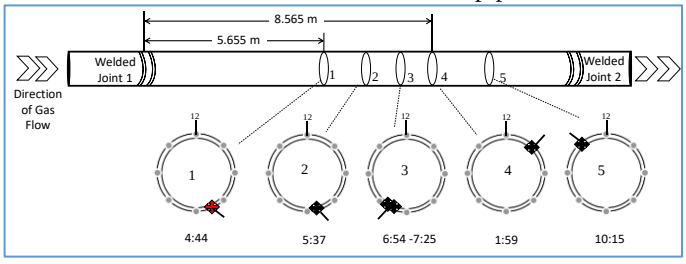

Fig.2 Single Line Diagram indicating the five locations of coating damage due to the Lightning Strike

The metal wall fusion and gas leakage had been identified, at location 1, as a hole with a conical shape. This damage is clearly shown in Fig. 3. The diameter of the hole at the surface of the coating was circular in shape with a diameter of 6.7 mm along the length of the pipeline and 6.2 mm along its circumference. On the inner surface of the coating, there was a bigger footprint (28 mm along the length and 27 mm along the circumference). The diameter of the hole associated with the metal wall fusion (location 1) has been measured to be approximately 2.3 mm.

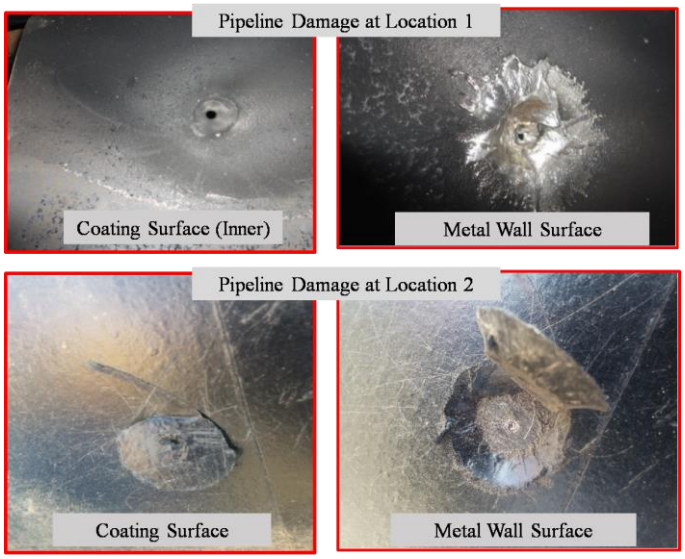

Fig.3 Pipeline Damage at two Different Locations

In the remaining four locations (2-5), there were evident marks of coating damage, as well as small damage on the external surface of the metal wall. The dimensions of this damage, for location 2 in particular, were 15 mm along the length, 18 mm along the circumference and the depth of the defect was 0.65 mm. A characteristic photo of the damage at location 2 is also shown in Fig. 3.

III. Laboratory Based Tests

A. Experimental Procedure and Objectives

The laboratory experiments carried out for this case study, reflect on some details and definitions described in the IEC 62305-1 [13]. It is thus important to quote that a downward lightning flash may consist of a first impulse (i.e. short stroke) and it may be followed by a long stroke (i.e. "part of the lightning flash that corresponds to a continuing current"). To this extent, the IEC 62305-1 [13] explicitly defines: a) the Impulse Charge (Q_{short}) as the value resulting from the time integral of the lightning current in an impulse and b) the long stroke charge (Q_{long}) as the value resulting from the time integral lightning current in a long stroke. As per the clauses of IEC 62305-1, the tests for the short or the long strokes can be applied on the test specimens separately, or as a combined test - where the long stroke follows the first impulse instantaneously.

Thus, the main objectives of the laboratory based testing were to simulate the specific energy of the first impulse (Q_{short}) and the charge of the long stroke (Q_{long}), on some specimens of the exact pipeline that had suffered the reported metal wall fusion (See Table I). More explicitly, the test results were used to elaborate on the hypothesis that it is mainly the Q_{long} that is capable of fusing the pipe metal wall. To this end, previous laboratory testing [14]-[15] has revealed that the long stroke charge is the dominant factor for metal fusion. Moreover, the work reported in [16] has noted the poor simulations of damage on airplane wings from the impulse current. It has nevertheless confirmed that severe damage can be attributed to large charge transfers that occur during the long-duration of lightning discharges (i.e. the continuing current phase). Finally, in [17], [18] a lightning arc test for Optical Ground Wires (OPGW) is described. The purpose of this test is to subject OPGW to lightning conditions that represent field conditions, in order to verify their mechanical performance. Of particular note to this end, is the fact that the lightning test parameters in [17] conform to charge transfers that result from the continuing current phase of a lightning flash.

1) Description of Test Specimens

To facilitate the investigation, a number of test specimens were extracted/cut from the circumference of a full ring pipeline unit. Each extracted specimen had dimensions of 150×150 mm. The metal wall of thickness of each specimen was 10 mm and the coating thickness was 5 mm (see Fig. 4). In the interest of space, this paper hosts the test procedures and results for three specimens only (D_1, D_2 and D_3).

2) Description of Test Procedure and Equipment

Two of the specimens (D_1, D_2) underwent a thorough process of preparation that involved accelerated environmental aging and some discrete artificial damaging on the coating material. The third specimen (D_3) was not subjected to any preparation/aging process. The preparation processes are briefly documented in Table V while the test specimens are shown in Fig. 4.

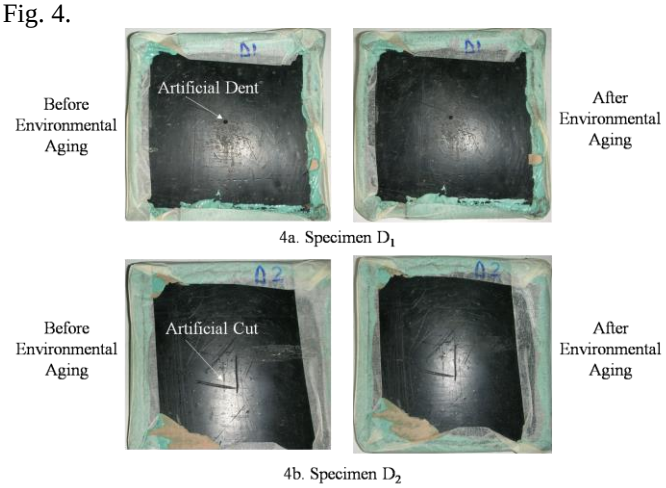

4a. Specimen D_1

4b. Specimen D_2

Fig.4 Photos of Test Specimens before and after the Environmental Ageing Process

The artificial damaging on the coating material (for specimens D_1, D_2) had been enforced before the accelerated environmental aging process. The latter has been achieved using an environmental chamber for salt mist ageing and an environmental chamber for humid sulphurous atmosphere ageing.

Following the completion of the preparation process, each specimen has been singly and consecutively subjected to the two stress tests described in Table VI. The experimental arrangement is shown in Fig. 5. In particular, Fig. 5 illustrates

the connection of the test-specimen to the output of the impulse current generator, via a pin brazed copper wire of 25 mm^2.

TABLE V
BRIEF DESCRIPTION OF SPECIMENS' PREPARATION

Test Specimen	Accelerated Environmental Aging	Artificial Damage on Coating
D_1 & D_2	1. Salt mist treatment (3 days) according to IEC EN 60068-2-52:2017 [19] 2. Humid sulphurous atmosphere treatment (7 days) according to EN ISO 6988:1985 [20]	D_1: Dent (Φ3,5 ×1 mm) on Coating (See Fig. 4a) D_2: Cut (1 mm Depth) on Coating (See Fig. 4b)
D_3	No Accelatered Aging Process has been applied	None

Fig.5 Attachment of the Test Specimen

It is worth noting that due to practical constraints, the DC follow test (#2) has been performed approximately 15 minutes after the impulse current test. However, it should be appreciated that this time delay, erred on the side of requiring high Q_{long} values for fusing the metal wall of the specimen. This is because any heat gained from the lightning impulse test was allowed to convect through the air.

TABLE VI
DESCRIPTION OF ELECTRICAL TESTS AND EQUIPMENT

	Test Description	Remarks
#1	Lightning Impulse Current Test	Each specimen (D_1-D_3) was stressed to a lightning impulse current pulse 10/350 μs, 100 kA of peak magnitude (I_{imp}), and specific energy (W/R) of approximately 2500 kJ/Ω.
Test # 1 has been performed through the use of a Lightning Impulse Current Generator 100kA, 65C, 187kJ. This test has been performed to simulate the Impulse Charge (Q_{short}) on the pipeline specimen.		
#2	DC follow Current Test	Each specimen (D_1-D_3) was stressed to a DC current pulse having a mean value of approximately 500 A for a time duration of 0.6 - 2.4 s.
Test # 2 has been performed through the use of a DC Voltage Generator 20kW, 625A. This test has been performed to simulate the long stroke charge (Q_{long}) on the pipeline specimen		

Note: The following two elements were used in the testing:
a) Resistive Impulse Shunt 1mΩ,100 kA, 2500kJ/Ω
b) Digital Oscilloscope 400MHz, 20 Gs/sec

3) Summary of test results

The results pertaining to the performed tests are summarized in Table VII. Moreover, the recorded damage on the specimens (D_1-D_3) upon the completion of each test is illustrated in Figures 6 – 8 respectively.

TABLE VII
SUMMARY OF TEST RESULTS

#1. Impulse Current Test (Q_{short})			
	D_1	**D_2**	**D_3**
Peak Current	99,9 kA	99,2 kA	101,3 kA
Specific Energy	2112 kJ/Ω	2017 kJ/Ω	2010 kJ/Ω
Charge	44,76 C	44,14 C	44,24 C
	Performed at the point of artificial coating damage	Performed at the point of artificial coating damage	Performed at the center of the specimen
#2. DC Follow Current Test (Q_{long})[1]			
	D_1	**D_2**	**D_3**
Current	520 A	520 A	460 A
Duration	1,2 s	1,2 s	2,34 s
Charge	624 C	624 C	1078 C
Recorded Damage Upon the completion of all tests			
	D_1	**D_2**	**D_3**
	Bore on the specimen (Full Penetration) (See Fig. 6)	Cavity with Dimensions: 5.2×4.5 mm 3.4 mm depth (See Fig. 7)	Bore on the specimen (Full Penetration) (See Fig. 8)

D_1 Upon Completion of the Impulse Current Test **D_1 Upon Completion of the DC Follow Test**

Fig.6 Recorded Damage on Specimen D_1 upon completion of stress tests

D_2 Upon Completion of the Impulse Current Test **D_2 Upon Completion of the DC Follow Test**

Fig.7 Recorded Damage on Specimen D_2 upon completion of tests

[1] To deduce the charge (Q_{long}) required to achieving a bore on the specimen (i.e. D_1 and D_3) the DC follow test has been performed on multiple samples of each specimen. For a selected number of tests, the current was kept constant but the time duration of each test was varied in steps of 0.02 s until the bore on the specimen was visually evident.

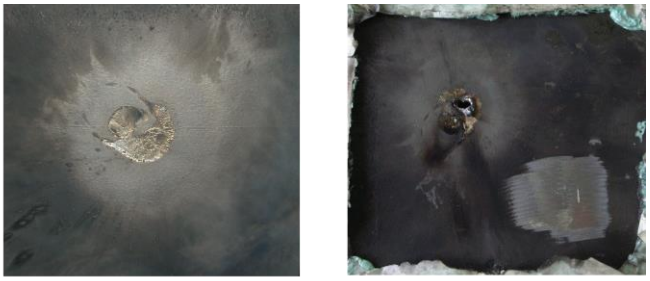

D_3 Upon Completion of the Impulse Current Test | **D_3 Upon Completion of the DC Follow Test**

Fig.8 Recorded Damage on Specimen D_3 upon completion of tests

4) Critical Evaluation of Test Results and Conclusions

The main conclusions drawn from the test results are listed as follows:

1. The conclusion from the impulse current tests - which had the objective to simulate the specific energy of the first impulse (i.e. short stroke) – is that, the Impulse Charge (Q_{short}) is not by itself adequate to cause fusion of the metallic wall of the pipeline. This conclusion is also shared by [16] for the case of aerospace vehicles. The lightning impulse can, however, create a severe damage on the coating material as well some defect on the outer surface of the metallic wall of the pipeline.
2. The main objective of the DC follow tests was to verify that the long stroke charge (Q_{long}) is capable of fusing the pipe metal wall. Thus, the test has been applied to D_1 to determine the charge required to fully melt the 10 mm wall thickness of the specimen. This charge was 624 C. This value of charge, although higher than the charge given in IEC-62305-1 [13] (Q_{long} = 200 C ± 20 % tolerance and T_{long} is 0.5 s ± 10 %), is not unrealistic. Charges higher than 624 C (resulting from the amplitude and the duration of the continuing current)[2] are reported in a CIGRE report [21] that describes lightning parameters for engineering applications. [Note: The CIGRE report explicitly dictates that: "*The continuing currents transfer higher charges compared to the impulse currents of the return strokes. Therefore, the continuing currents are the main source for burning holes into metal plates"*]

Moreover, the same 624 C charge was then applied to D_2 and the conclusion was that the metallic wall was partly melted (i.e. cavity with dimensions: 5.2×4.5 mm, 3.4 mm depth). The difference in the two tests lies in the fact that the artificial coating damage on specimen D_1 was more severe (i.e. the metal wall was exposed and lightly damaged) than the artificial coating damage on D_2. Therefore, D_2 would require more charge to achieve a complete metal wall fusion. To verify the fact that the condition of the coating can influence the charge required to cause metal wall fusion, the test has been applied to specimen D_3. It is reiterated at this point that D_3 has not been subjected to any accelerated aging process and no artificial damage has been enforced on its coating material. Therefore, the latter test has concluded that metal wall fusion can occur at a charge value of 1078 C.

To this end, the generic conclusion that can be drawn from the DC follow tests (irrespective of the absolute Q_{long} charge) is that when pre-existing defects are present on the pipeline (on the coating and metallic wall) the Q_{long} charge required to cause metal wall fusion is much less than the charge required for a pipeline free of defects (i.e. just after its installation).

[2] Within the CIGRE report [21] the Q_{long} values can be correlated to cumulative probability distributions for a) continuous current magnitudes and b) current durations for both positive and negative strokes.

IV. Further Investigation - Modelling

By virtue of the reported damage (i.e. the pipe metal wall fusion) and by reviewing the field investigation findings (Section II), it is rational to assume that the direct flash episode has forced a high current-discharge to pass on the pipeline's metal wall. Moreover, the laboratory tests carried out (Section III), have confirmed that it is the long stroke (i.e. "part of the lightning flash that corresponds to a continuing current") that is capable to cause the metal wall fusion. However, it was also concluded that the level of Q_{long} required to cause fusion depends on the presence of existing defects on the pipeline's coating and metal layers.

Thus, the primary objective of this section is to further understand this process, through modelling activities. In particular, the modelling pertains in investigating whether the soil ionization can act to facilitate the flow of the long stroke (i.e. "part of the lightning flash that corresponds to a continuing current") directly into the pipeline's metal through existing coating defects. It is noted that the modelling investigation in this paper is limited to simulating the long stroke, since it was experimentally verified that it is the dc component associated with the long stroke that is able to cause metal wall fusion. To this extent, the modelling endeavor consists of the following stages: a) design of a full-scale topologically accurate pipeline model, b) development and integration of a coating defect model, c) soil ionization model and dc energization principles, d) simulation and post-processing of results.

A. Development of Full Scale Simulation Model

Figure 9 illustrates the top plan view of the developed geometrically accurate simulation model. This was achieved through the use of CDEGS software [12].

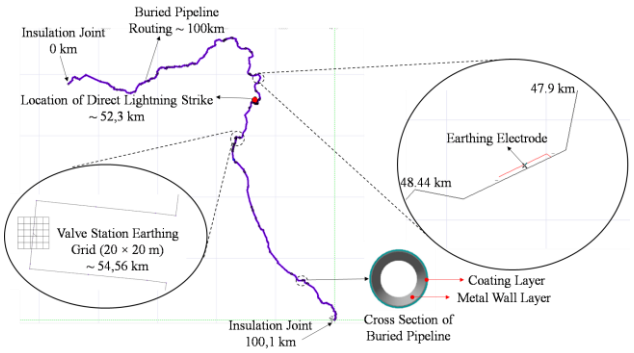

Fig.9 Layout of Scale Simulation Model in CDEGS software

The characteristics of the pipeline (i.e. material specifications, size, earthing electrodes, insulation joints) that are used in the simulation model, are those provided in

Section II-A. Further to the data described in Section II-A, for the subsequent simulations, the spark gap across the insulation joint, located at 61.336 km, is bridged (i.e. it was assumed that the voltage across the insulation joint exceeds its rated impulse spark over voltage - 2.2 kV (Table II), under the reported lightning strike location).

B. Development and Integration of an Equivalent Coating-defect Model

1) Relevant Literature Survey

The AUS standard [3] dictates that it is sensible to assume that a coating defect can occur anywhere on a pipeline and not use the existence of a pipeline coating as defense. As noted in [22], coating defects on buried pipeline systems can be caused from an earth fault at a transmission line tower, close to the pipeline. As a result, the pipeline's coating may be left weakened/damaged and thus susceptible to further detrimental deterioration. Moreover, severe damage on the pipelines' coating can occur due to direct lightning strikes in the immediate vicinity. To support this argument, the field investigation findings presented in section II-B (Fig. 2) have confirmed that a direct lightning strike, near the pipeline, can adversely damage its coating material and to some extent, its metal wall layer (see Figure 3b).

2) Coating Defect Model

To study the impact of coating defects on the pipeline's susceptibility to lightning strikes, an equivalent coating defect model has been developed. This model has been integrated in the simulation model, as shown in Fig. 10.

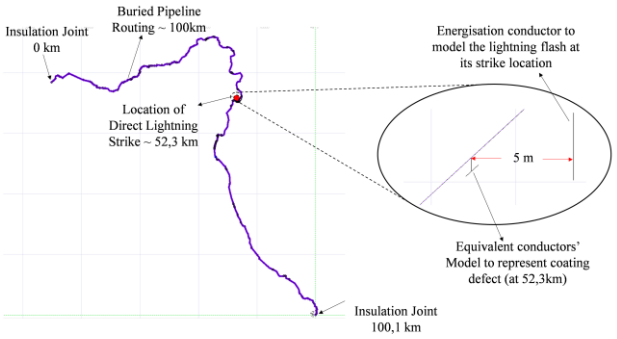

Fig.10 Integration of a Coating Defect in the Simulation Model

To achieve this, it was assumed that the pipeline has a small cylindrical coating defect of an equivalent area of 1 cm^2. The resistance to earth (R_d) of this coating defect can be calculated as $R_d = \frac{\rho}{4r}$ [23] where ρ is the local soil resistivity and r is the radius of the cylindrical defect. Depending on the value of the local soil resistivity and on the size of the assumed coating defect, the value of R_d can be determined. In the simulation model, the coating defect (R_d) is integrated by means of equivalent conductors, which are appropriately sized and calibrated to match the calculated R_d. It is noted that the coating defect model has been integrated in the simulation model, at the location where the pipeline, has suffered the metal wall fusion (i.e. 52nd km).

C. Soil Ionization Model and Energization Principles

1) Relevant Literature Survey

Many theoretical and practical studies suggest that when an impulse current is injected into the soil, the high current density in the vicinity of the injection point, can locally increase the soil's electric field [4]-[10], [24]-[30]. This increase has the effect of producing a local ionization zone in the soil. To this end, some experimental studies [5], [8], [10], [24]-[30] have shown that if this electric field exceeds some critical value (E_c), then soil breakdown can occur. We note however, that the soil is an inhomogeneous medium with subcomponents that include: a) solid soil particles, b) ionic liquid and c) humid-air. The mixture of solid, air and liquid elements results in a non-linear electrical conductivity [27]. Therefore, depending on the soil composition, the critical value of electric filed gradient (E_c) for soil breakdown can range between 300-1850 kV/m [4]-[5], [24]-[26]. In practice, due to the inhomogeneous soil's nature, the ionization zone that is formed into the soil can have an arbitrary shape [24], [27], [30]. However, the ionization zone can be conveniently considered to be hemispherical [5], [8], [10], under the assumption that the lightning current can be radially dissipated in a homogeneous soil (ρ). In such case, the radius (R_{ion}) of the ionized hemisphere for a homogeneous soil can be calculated as given in (1). Within (1), I_m is the maximum lightning current [1] and E_c is the critical value of electric field for which soil breakdown can occur [1], [10]. This implicitly entails that all metallic objects within the ionized zone will be attached by arcs formed in the soil.

$$R_{ion} = \sqrt{\frac{I_m * \rho}{2\pi * E_c}} \qquad (1)$$

It is nevertheless highlighted that in the ionized region, the soil resistivity can follow some dynamic hysteresis loop profile [7]-[9]. As described in [8] the soil resistivity value will remain constant before the critical value of electric filed (E_c) is reached. When E_c is exceeded, the ionization process commences and the value of the soil resistivity decreases, as the current density continues to grow. The residual resistivity in the soil ionization region, is considered to be 7% [29] or in the order of 0.001 – 0.003% of the original soil resistivity [30]. As indicated in [7]-[9], the residual soil resistivity can be sustained for some time before starting to gradually restore back to its initial value. The restore time is reported in [27] to be proportional to the impulse current amplitude that produces the ionization of the soil.

2) Equivalent Soil Ionization Model

For a uniform soil resistivity structure, the ionization radius (R=R_{ion}) of a hemispheroidal zone can be computed using (1). To this end, Fig. 11 shows a sensitivity analysis for R_{ion} with respect to different E_c values under three discrete I_m scenarios (31 kA, 100 kA and 200 kA). In all scenarios, the soil resistivity was assumed uniform (i.e. 1535.51 Ωm). As evident in Fig. 11, R_{ion} depends on the maximum lightning current I_m and on the critical value of electric field E_c to allow for soil breakdown.

However, in this study a more rigorous approach has been followed to estimate an appropriate R_{ion} value. The approach followed, reflects: a) on the three-layer soil structure reported in Table IV (resulted from field

measurements), b) on a maximum lightning current I_m and c) on a critical value of electric field E_c to allow for soil breakdown.

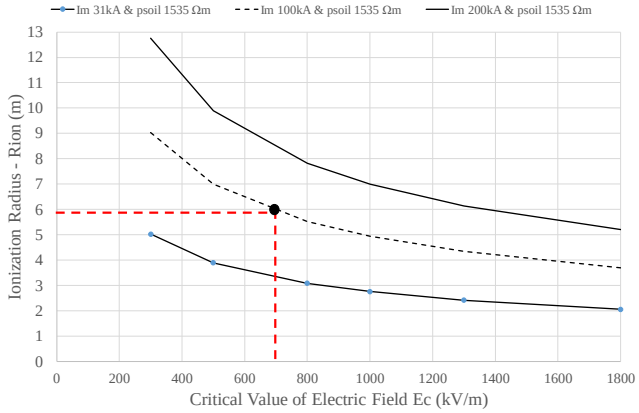

Fig.11 Sensitivity Analysis for R_{ion} (Uniform soil resistivity conditions)

In particular, the R_{ion} calculation relies on a series of parametric simulations using CDEGS software. The process initially involves injecting a lightning impulse current (I_m) at the ground surface of the three-layer soil model (Table IV). Following this injection, the voltage gradient (kV/m) that develops within the three-layer soil structure, is calculated through a build-in method (HIFREQ/FFTSES) that obtains the electromagnetic fields in the time domain, from a corresponding frequency domain response based on the shape of the lightning impulse current (I_m) [12].

The calculation of the voltage gradients conforms to 50 discrete circular surfaces, which are vertically distributed (i.e. every 0.10 m) across the depth of the 3-layer soil structure (Table IV). Thus, for each surface an equivalent R_{ion} is determined, according to a specified critical value of electric field E_c that is set as a boundary condition. The simulation results are shown in Fig. 12, for an E_c value of 700 kV/m and I_m 100 kA 10/350 μs.

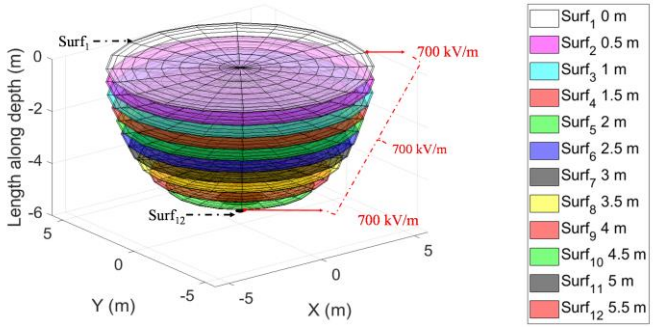

Fig.12 Calculated Soil Ionization Zone for the 3-layer soil structure (Table IV) for I_m*100* kA and E_c *700* kV/m

We highlight that in this particular study, the 700 kV/m threshold was assumed to apply across the entire three-layer soil structure. This is a rational assumption since the combined depth of the two upper soil layers is only 1.14 m. Effectively, the dominant soil layer is the third one (1535.51 Ω.m for infinite depth). [Note: The pipeline is laid on the third soil layer].

For completeness, a comparison with regard to the ionization zone formed in the three-layer soil structure and in the uniform 1535.51 Ωm soil structure is shown in Fig. 13. The conclusion from this comparison is that for the three-layer soil structure, R_{ion} at the ground surface, is reduced to 5.8 m (Fig.12) when compared to the 5.9 m R_{ion} value corresponding to the uniform soil structure (Fig. 11). A further conclusion is that the ionisation zone in the three-layer soil structure is not entirely hemispheroidal and thus, its calculated ionized volume is 4.47 % less than the ionized volume - calculated for the uniform soil structure (i.e. 1535.51 Ωm).

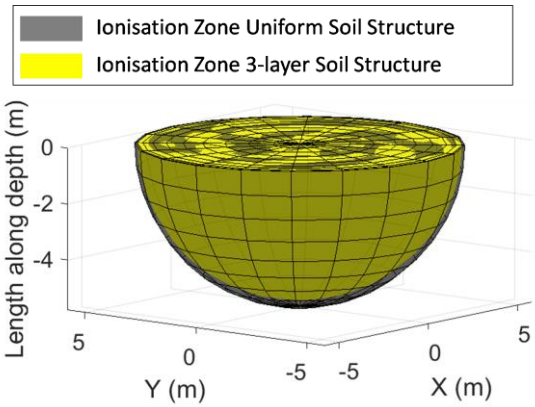

Fig.13 Comparison of Ionized Soil Zones: Three-Layer Soil Structure Vs Uniform Soil Structure (for I_m 100 kA and E_c 700 kV/m)

Following the above remarks, the soil ionisation effects are integrated in the simulation model, through a build-in soil model (see Fig. 14) of the software.

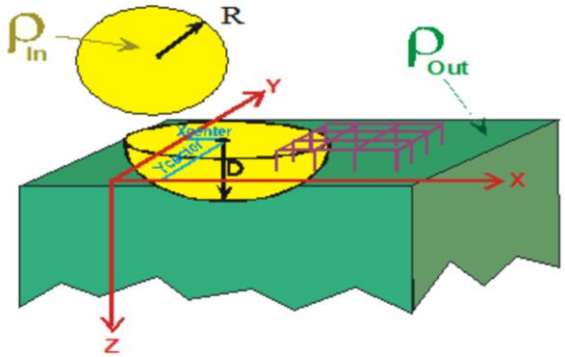

Fig.14 Hemispheroidal Soil Model – MALZ/CDEGS [12]

This approach accounts for the fact that the ionization can be modelled by two-part soil models [8], [31]-[32]. The first part accounts for the non-ionization zone (i.e. the soil has its original value of resistivity - ρ_{out})[3] and the second accounts for a hemispheroidal ionization zone (i.e. the soil has a residual value of resistivity - ρ_{in}). For this case study, an E_c value of 700 kV/m has been used, as a conservative

[3] In this simulation, ρ_{out} was assumed to be equal to 1535.51 Ωm. This soil resistivity corresponds to the bottom of the three-layer soil structure (Table IV) i.e. the layer at which the pipeline is laid.

value. Moreover, the dimensions (i.e. volume) of the ionized zone were set as per the results provided in Fig.12, for the three-layer soil structure. These input parameters ensure that the pipeline (and its coating defect) will fall into the ionisation zone. This is illustratively shown in Fig. 15. [Note: It was assumed that the center of the ionized hemisphere coincides with the lightning injection point into the soil].

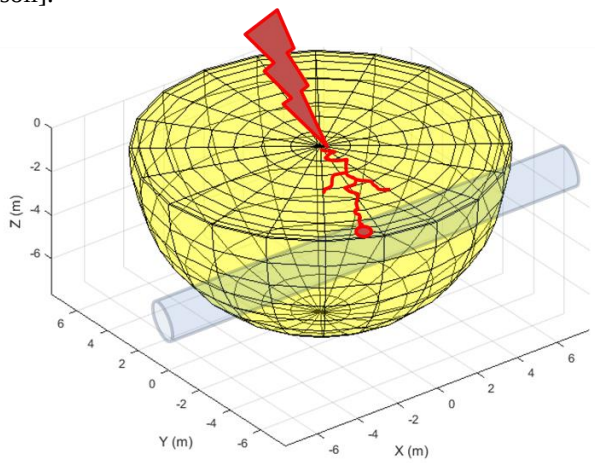

Fig.15 Illustrative plot: Pipeline routing falling within ionization zone

3) Energization of the Simulation Model

With reference to Fig. 10, the simulation model is energized by means of a conductor that is modeled as a current source. The conductor can be energized by a lightning transient or a dc pulse to discretely emulate the effects of Q_{short} or Q_{long} on the pipeline. (Note: In the simulation model, (see Fig. 10) a direct current is injected into the soil at a 5 m distance from the modelled coating defect. This is to reflect on the field investigation findings described in Section II-B).

4) Summary of Input Parameters

Following all the remarks documented in Section IV, the input parameters employed in the simulation process are summarized in Table VIII.

TABLE VIII
INPUT PARAMETERS

Ionized Soil Resistivity Model		
Description	***Value***	***Remarks***
Soil resistivity of non-ionization zone	ρ_{out} =1535.51 Ω.m	It reflects on the soil resistivity layer the pipeline is laid on
Soil resistivity of ionization zone	ρ_{in} =1.53 Ω.m	Assumed value: 0.1% of original soil resistivity
Critical value of electric filed gradient (E_c)	700 kV/m	It may range between 300-1850 kV/m [4]-[5]
Dimensions of hemispheroidal ionization zone	Figure 12	Resulting from the three-layer-soil structure (Table IV)
Coating Defect Model		
Description	***Value***	***Remarks***
Equivalent area of coating defect	A=$\pi \times r^2$=1cm^2	The coating defect is assumed to have a cylindrical shape.
Equivalent resistance to earth of coating cylindrical defect	$R_d = \frac{\rho}{4r}$	Depends on the local soil resistivity and on the size of the coating defect.
Energization - Long Stroke		
Description	***Value***	***Remarks***
Long Stroke: part of the lightning flash that corresponds to a continuing current	I_{dc}=400 A	Q_{long} as per IEC 62305-1 is 200 C [13] Q_{long} as per IEEE Standard 1138-2009 can be 400 A for 0.5 s [17]

D. Simulation and Post-Processing of results

1) Solution Method

The following simulation results pertain to a numerical solution that relies on the use of the MALZ computation module of CDGES [12]. This module relies on a hybrid method for calculating responses from grounding systems, namely, a quasi-static approximation of Maxwell equations [33]-[35].

2) Simulation Results

Figure 16 illustrates the simulation results for the current that is entering the pipeline through the coating defect. It is shown that when soil ionization is considered, 178 A out of the 400 A dc that is injected into the soil, enters the pipeline through the coating defect. That is 659 times higher than the current entering the pipeline when no soil ionization is considered (i.e. 0.27 A out of 400 A dc).

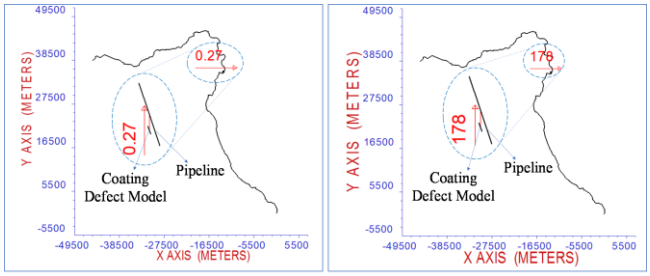

a. Uniform Soil Model
ρ_{in}=ρ_{out}=1535.51 Ω.m

b. Ionized Soil Model
ρ_{out}=1535.51 Ω.m & ρ_{in}=1.53 Ω.m

Fig.16 Current entering the pipeline through the Coating Defect

To this end, Fig. 17 shows a sensitivity analysis that captures the dependency of the current entering through the coating defect under varying values of the ionized residual resistivity (i.e. ρ_{in}). The conclusions from this analysis is that the amount of current entering the pipeline depends: a) on the magnitude of the dc component of the long stroke and b) on the local soil resistivity value of the ionized zone.

To further investigate the thermal effects on the pipe metal wall, at the location where the current enters the pipeline through the coating defect, the anode-or-cathode voltage drop model described in Annex D of the IEC 62305-1 [13] is used. This model provides conservative results for the volume (V) of melted metallic material under a ligniting discharge event. This is mathematically described in (2) [13]. The conservatism arises from the assumption that all the energy injected through the defect is used to melt the conductive material by neglecting the heat diffusion within the metal.

$$V = \frac{U_{a,c} \times Q}{\gamma \times (C_w \times (\theta_s - \theta_u) + C_s)} \quad (2)$$

A desciption of the parameters shown in (2) as well as the values used in the calculation are documented in Table IX. To this extent, Fig. 18 shows the calculated volume of melted metal for different cathode voltage drops ($U_{a,c}$). The analysis has been

performed for Q=89 C. The 89 C has been deduced since the current through the coating defect was calculated equal to 178 A (see Fig.15). Thus, assuming a time duration of 0.5 s as prescribed in [13], [16], the value of Q is approximately equal to 89 C. With reference to Fig. 18, we take (as an example) the volume of melted metal (167 mm^3) calculated for a cathode voltage drop equal to 14 V. If we were to transfer this volume to an equivalent circular truncated cone with height 10 mm (i.e. equal to the thickness of the pipe metal wall) the diameters of the trancated cone would be 2.3 mm (upper surface) and 6.6 mm (lower surface). Thus, these values are comparable to the diametre of the conical shape hole that deduced from the field investigation of the real incident (see Section II-B) . Therefore, this confirms that it is possible to have metal wall fusion when the conditions described and simulated in Section IV are met.

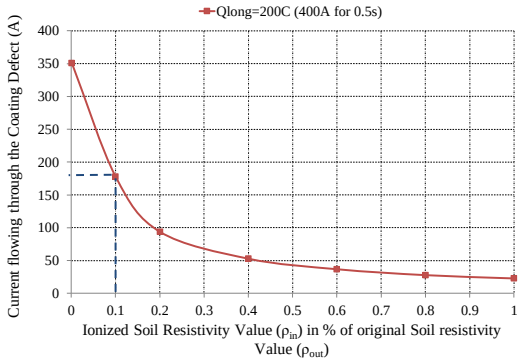

Fig.17 Sensitivity Analysis for current entering through the coating defect when Soil Ionization is considered

TABLE IX
INPUT PARAMETERS FOR CALCULATION OF MELTED METAL

Parameter	Description	Value
Q (C)	Charge of the ligthning current	Q=178A×0.5s=89 C
$U_{a,c}$ (V)	cathode voltage drop[1]	In the order of a few tens of Volts [13],[36]
γ (kg/m^3)	material density[1]	7700
C_w (J/kgK)	thermal capacity[1]	469
θ_s (°C)	melting temperature[1]	1530
θ_u (°C)	ambient temperature	25
C_s (J/kg)	latent heat of melting[1]	272×10^3
[1] The data used are obtained from Table D2 of IEC 62305-1 [13] and they refer to mild steel material.		

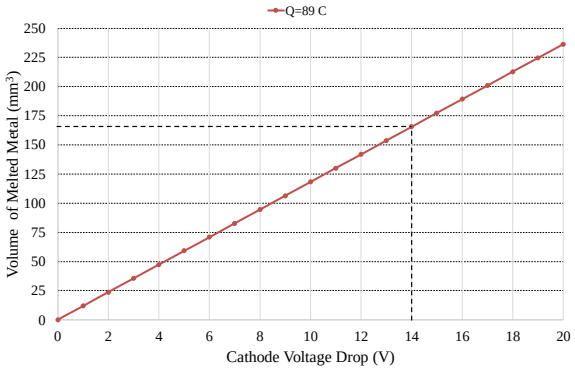

Fig.18 Volume of Melted Steel Metal under Different Cathode Voltage Drop Values

V. DISCUSSION OF RESULTS AND CONCLUSIONS

The paper has presented a documented wall fusion incident on an underground Gas Transmission System, due to a nearby direct lightning strike. The work embraces a field investigation report as well as in-house laboratory experiments and modelling activities. The main conclusions that are drawn from these endeavors are as follows: Depending on the type of lightning current, the corresponding charge (Q_{flash}) may involve the charge of the short stroke Q_{short} and the charge of the long stroke Q_{long}. The laboratory tests have confirmed that it is the long stroke (i.e. "part of the lightning flash that corresponds to a continuing current") that is capable to cause the metal wall fusion. However, it was also concluded that the level of Q_{long} required to cause fusion depends on the presence of existing defects on the pipeline's coating and metal layers.

Moreover, in the event of a direct lightning strike near a buried pipeline, a high value of electric field can be generated in the immediate vicinity of the lightning current discharge location. If this value of electric field exceeds the value of the "ground ionization gradient", it may cause the influenced area of soil, to behave very conductively (i.e. soil breakdown). If the pipeline's routing falls within the formed ionization zone, then the lightning discharge current can enter the pipeline through the pre-existing coating defects that they also fall within the ionization zone. Thus, the presence of a preexisting coating defect can drain the long stroke charge Q_{long} to flow through the pipeline's coating to reach its metal wall. These defects make the pipeline conductance to earth greater than that of a well-insulated section. Because the current enters the pipe through an imperfection in the coating, the current density at the defect's location is high, even for humble current values, since the size of a defect is usually microscopic. This flow can cause intense localized heating and subsequent pipe wall fusion if all the necessary conditions are met.

REFERENCES

[1] P. Venturino, J.N. Booman, M.O. Gonzalez, J.L. Otegui, "Pipeline failures due to lightning", *Engineering Failure Analysis*,Vol. 64, pp. 1-12, June 2016.
[2] Joseph Pikas, William Shoaf, "The lightning threat to pipelines and coatings", *J. Pipeline Eng.*, Vol. 9, pp. 191–196, Sep. 2010
[3] *Electrical hazards on metallic pipelines*, AS/NZS 4853, 2012.
[4] E. E. Oettle, "A new general estimation curve for predicting the impulse impedance of concentrated earth electrodes," in *IEEE Transactions on Power Delivery*, vol. 3, no. 4, pp. 2020-2029, Oct. 1988.
[5] G. M. Petropoulos, "The high-voltage characteristics of earth resistances," in *Journal of the Institution of Electrical Engineers - Part II: Power Engineering*, vol. 95, no. 43, pp. 59-70, Feb. 1948.
[6] J. Cidras, A. F. Otero and C. Garrido, "Nodal frequency analysis of grounding systems considering the soil ionization effect," in *IEEE Transactions on Power Delivery*, vol. 15, no. 1, pp. 103-107, Jan. 2000.
[7] S. Sekioka, M. I. Lorentzou, M. P. Philippakou and J. M. Prousalidis, "Current-dependent grounding resistance model based on energy balance of soil ionization," in *IEEE Trans. on Power Del.*, vol. 21, no. 1, pp. 194-201, Jan. 2006.
[8] A. C. Liew and M. Darveniza, "Dynamic model of impulse characteristics of concentrated earths," in *Proceedings of the Institution of Electrical Engineers*, vol. 121, no. 2, pp. 123-135, February 1974.
[9] M. Mokhtari and G. B. Gharehpetian, "Integration of Energy Balance of Soil Ionization in CIGRE Grounding Electrode Resistance Model," in *IEEE Transactions on Electromagnetic Compatibility*, vol. 60, no. 2, pp. 402-413, April 2018.
[10] Junping Wang, A. C. Liew and M. Darveniza, "Extension of dynamic model of impulse behavior of concentrated grounds at high currents," in *IEEE Tranç. on Power Del.*, vol. 20, no. 3, pp. 2160-2165, July 2005.

[11] Lagouvardos, K., Kotroni, V., Betz, H.D., Schmidt, K., 2009. A comparison of lightning data provided by ZEUS and LINET networks over Western Europe. Nat. Hazards Earth Syst. Sci. 9 (5), 1713–1717.
[12] CDEGS Software, Safe Engineering Services & Technologies Ltd Montreal, Quebec, Canada Est. 1978.
[13] *Protection against lightning - Part 1: General principles*, IEC std. 62305-1, 2010
[14] Kern, Alexander, "Simulation and measurement of melting effects on metal sheets caused by direct lightning strikes", NASA. Kennedy Space Center, *The 1991 International Aerospace and Ground Conference on Lightning and Static Electricity*, Volume 1; p. 10.
[15] M. Iwata, T. Ohtaka, M. Kotari and Y. Goda, "Breaking Characteristics of 60 mm^2OPGW Strands due to DC Arc Simulating High-Energy Lightning Strike," *2018 34th International Conference on Lightning Protection (ICLP)*, Rzeszow, 2018, pp. 1-4.
[16] C. C. Goodloe, "Lightning Protection Guidelines for Aerospace Vehicles", Marshall Space Flight Center, National Aeronautics and Space Administration, MSFC, Alabama 35812, May 1999 [Available Online: https://ntrs.nasa.gov/archive/nasa/casi.ntrs.nasa.gov/20000004589.pdf].
[17] IEEE 1138-2009 - IEEE Standard for Testing and Performance for Optical Ground Wire (OPGW) for Use on Electric Utility Power Lines, Published Date: 2009-11-30.
[18] M. Iwata, T. Ohtaka, Y. Kuzuma and Y. Goda, "Development of a Method of Calculating the Melting Characteristics of OPGW Strands Due to DC Arc Simulating Lightning Strike," in *IEEE Transactions on Power Delivery*, vol. 28, no. 3, pp. 1314-1321, July 2013.
[19] *Environmental testing - Part 2-52: Tests - Test Kb: Salt mist, cyclic (sodium chloride solution)*, IEC std. 60068-2-52, 2017.
[20] *Metallic and other non organic coatings -- Sulfur dioxide test with general condensation of moisture*, ISO std. 6988, 1985
[21] GIGRE Technical Brochure 549, Lightning Parameters for Engineering Applications, Working Group C4.407, August 2013.
[22] GIGRE Technical Brochure 290, AC corrosion on metallic pipelines due to interference from ac power lines,Joint Working Group C4.2.02 , April 2006.
[23] *Protection against corrosion by stray current from direct current systems*, EN std. 50162, 2004.
[24] W. Sima, S. Liu, T. Yuan, D. Luo, P. Wu and B. Zhu, "Experimental Study of the Discharge Area of Soil Breakdown Under Surge Current Using X-Ray Imaging Technology," in *IEEE Trans. on Industry App.*, vol. 51, no. 6, pp. 5343-5351, Nov.-Dec. 2015.
[25] J. He, B. Zhang, R. Zeng and B. Zhang, "Experimental Studies of Impulse Breakdown Delay Characteristics of Soil," in *IEEE Transactions on Power Delivery*, vol. 26, no. 3, pp. 1600-1607, July 2011.
[26] I. F. Gonos and I. A. Stathopulos, "Soil ionisation under lightning impulse voltages," in *IEE Proceedings - Science, Measurement and Technology*, vol. 151, no. 5, pp. 343-346, 4 Sept. 2004.
[27] X. Wen *et al*., "Sparkover observation and analysis of the soil under the impulse current," in *IET Science, Measurement & Technology*, vol. 10, no. 3, pp. 228-233, 5 2016.
[28] P. Espel, R. R. Diaz, A. Bonamy and J. N. Silva, "Electrical parameters associated with discharges in resistive soils," in *IEEE Transactions on Power Delivery*, vol. 19, no. 3, pp. 1174-1182, July 2004.
[29] Yaqing Liu, N. Theethayi, R. M. Gonzalez and R. Thottappillil, "The residual resistivity in soil ionization region around grounding system for different experimental results," *2003 IEEE Symposium on Electromagnetic Compatibility. Symposium Record (Cat. No.03CH37446)*, Boston, MA, USA, 2003, pp. 794-799 vol.2.
[30] S. Liu, W. Sima, T. Yuan, D. Luo, Y. Bai and M. Yang, "Study on X-Ray Imaging of Soil Discharge and Calculation Method of the Ionization Parameters," in *IEEE Trans. on Power Del.*, vol. 32, no. 4, pp. 2013-2021, Aug. 2017.
[31] A. Geri, "Behaviour of grounding systems excited by high impulse currents: the model and its validation," in *IEEE Transactions on Power Delivery*, vol. 14, no. 3, pp. 1008-1017, July 1999.
[32] A. Habjanic and M. Trlep, "The simulation of the soil ionization phenomenon around the grounding system by the finite element method," in *IEEE Transactions on Magnetics*, vol. 42, no. 4, pp. 867-870, April 2006.
[33] F. P. Dawalibi and A. Pinho, "Computerized Analysis of Power Systems and Pipelines Proximity Effects," IEEE Transactions on Power Delivery, Vol. 1 No. 2, April 1986, pp. 40-48.
[34] F. P. Dawalibi and D. Mukhedkar, "Ground Electrode Resistance Measurements in Nonuniform Soils,"IEEE Transactions on Power Apparatus and Systems, Vol. PAS-93, No. 11, January 1974, pp. 109-115.
[35] D. Mukhedkar, Y. Gervais, and F. P. Dawalibi, "Modelling of Potential Distribution around a Grounding Electrode,"IEEE Transactions on Power Apparatus and Systems, Vol. PAS-92, No. 5, September/October 1973, pp. 1455-59.
[36] M. L. Rossi, V. Ponomarev and A. Scotti, "Heat Exchange and Voltage Drop in Welding Arc Column," in *IEEE Transactions on Plasma Science*, vol. 44, no. 10, pp. 2446-2454, Oct. 2016.

ACKNOWLEDGMENT

The work was financially supported by the Hellenic Gas Transmission System Operator (DESFA), under a project-based agreement. The practical work performed by the staff of ELEMKO's H.V. Laboratory (accredited according to EN/ISO-IEC 17025 and ISO 9001/2000) is sincerely acknowledged.

BIOGRAPHIES

Charalambos A. Charalambous is an Associate Professor, in the Department of Electrical and Computer Engineering, at the University of Cyprus. He is the founder and director of the Power System Modelling Laboratory. His current research interests include solar applications, DC and AC interference and corrosion evaluations in power system applications, earthing/grounding. He is an expert member of in the standardization committee ISO/TC 67/SC 2/WG 24 "DC stray current for Pipeline Systems".

Andreas Dimitriou received a MEng (Hons) degree in Electrical & Computer Engineering in 2013 National Technical of Athens (NTUA). He is a PhD candidate within the Power System Modelling Laboratory that operates under the ECE Department of the University of Cyprus. His main research interests include DC interference, grounding and lightning protection of large scale solar applications.

Nikolaos Kioupis is the Head of Inspection Section of the Hellenic Gas Transmission System Operator. He received his Ph.D. in Chemical Engineering from National Technical University of Athens (NTUA) in 2009.He is a pipeline integrity, cathodic corrosion protection and AC corrosion mitigation expert. He is also involved in surge/lightning protection and intrinsic safety of gas pipeline infrastructure facilities. He is a member of CeoCor (European Committee of Corrosion and Protection of Pipes and Pipeline Systems) since 2004. He has actively participated in working groups of CEN and ISO for the elaboration of technical standards on Cathodic Protection and AC corrosion.

Theagenis Manolis is currently working in the Department of Cathodic Protection and Surge/Lightning Protection at the Hellenic Gas Transmission System Operator S.A. (DESFA). He is a cathodic protection engineer, surge/lightning protection expert and inspection engineer of electrical and electronics facilities in the Inspection Section of DESFA. Since 2002 he has participated in projects and research items related to lightning and cathodic protection of natural gas pipelines.

Nikolaos D. Kokkinos received the M.Sc and Ph.D. degrees in High Voltage Engineering from UMIST in 2001 and 2004 respectively. He is now the C.E.O of ELEMKO, SA. He is a Chartered Engineer (C.Eng. –IET) and since 2007, he is an active member as an expert in 1) the International standardization committee IEC SC 37A, 2) in the European standardization committee CLC TC 37, and 3) in the European standardization committee CLC SC 9XC.